AJS American Journal of Science
publishing earth-sciences research since 1818

Chen, N. H.-C., Dong, Y., & Hui, B. (2024). Zircon U-Pb Age and Hf-O Isotope Evidence of the Taihua Complex on the Southern Margin of the North China Craton: Implications for Its Magmatic Process During the Early Paleoproterozoic. *American Journal of Science*, *324*, 14. https://doi.org/10.2475/001c.123684

Science Paper

Zircon U-Pb Age and Hf-O Isotope Evidence of the Taihua Complex on the Southern Margin of the North China Craton: Implications for Its Magmatic Process During the Early Paleoproterozoic

Nancy Hui-Chun Chen[1][a], Yunpeng Dong[2], Bo Hui[2]

[1] Department of Resources Engineering, National Cheng Kung University, [2] State Key Laboratory of Continental Dynamics, Department of Geology, Northwest University (China)

Keywords: Zircon U–Pb geochronology, Hf–O isotopes, Paleoproterozoic, Xiaoqinling terrane, Taihua Complex, North China Craton

https://doi.org/10.2475/001c.123684

American Journal of Science

Vol. 324, 2024

The Xiaoqinling is the largest terrane of the Taihua Complex and records Paleoproterozoic silicic magmatism, which is one of the most potential areas for understanding secular changes in tectonic processes during the Tectono-Magmatic Lull (TML). In this study, we use zircon U–Pb dating, Lu–Hf and O isotopic analysis to constrain the age, provenance, and magmatic processes of the protoliths for the Paleoproterozoic granitic gneiss, tonalitic gneisses, and migmatitized tonalitic gneiss from the Xiaoqinling area. The isotopic composition of zircon provides a key proxy for querying the crustal record. Integration of our new U–Pb and Hf–O isotope data with available published data from other regions of the North China Craton (NCC), allows us to better assess the secular changes of the North China Craton during the magmatic lull at ~2.3 Ga. This study shows that the protolith of the tonalitic gneisses in the study area have crust-like Hf–O isotopic compositions with slightly negative to positive εHf(t) (−3.0–+2.1) and low to moderately elevated $\delta^{18}O$ values (2.71–7.87‰), indicating a mixed origin of continental crust assimilated by mantle-derived magmas.

1. INTRODUCTION

A global-scale continental magmatism decreased during the Tectono-Magmatic Lull (TML, 2365–2235 Ma) (Condie et al., 2022) has attracted considerable attention. Although there were a few magmatic activities during this period, there is a relative scarcity in terms of silicic magmatism (SiO_2 > 65 wt%) (Partin et al., 2014; Scaillet et al., 2016; Teixeira et al., 2015). The North China Craton (NCC) (fig. 1) is one of the ancient cratons in the world, preserving older crustal remnants that date back to *circa* (*ca.*) 3.8 Ga in the eastern part of the craton (D. Y. Liu et al., 1992). It is noteworthy that the NCC witnessed early Paleoproterozoic silicic magmatism at *ca.* 2.3 Ga, and the tonalite-trondhjemite-granodiorite (TTG) suits formed in the Taihua complex of the southern margin of the Trans-North China Orogen (TNCO) (fig. 1) (Diwu et al., 2014; Huang et al., 2012; X.-L. Jia et al., 2019; G.-D. Wang et al., 2017; Yu et al., 2013). Geologists have carried out extensive field-based structural, petrological, geochemical, geochronological and geophysical investigations on the southern TNCO, and produced large amounts of data and competing interpretations. However, most of these investigations have focused on ages, structural, and tectonic evolution (Diwu et al., 2014; Huang et al., 2012; X.-L. Jia et al., 2019; Y. Li et al., 2018; X. Wang et al., 2019; Yu et al., 2013; Y. Zhou et al., 2016). Comparatively, less attention has been paid to magmatic processes that had been operative on the southern part of the TNCO. Oxygen isotopes have been extensively adopted in combination with petrological and geochemical data to determine magmatic processes, such as crystallization, evolution, and generation of magma (Taylor & Sheppard, 1986). Only a few oxygen isotope data have been reported for early Precambrian rocks in the southern NCC (Sun et al., 2023; X. Wang et al., 2021; Y. Zhou et al., 2021). The Xiaoqinling is the largest terrane of the Taihua Complex and records Paleoproterozoic magmatism (Diwu et al., 2014; Yu et al., 2013), which is one of the most potential regions for understanding of secular changes in tectonic processes during the ~2.3 Ga magmatic lull.

In this contribution, we report zircon U-Pb, Lu-Hf and O isotopic compositions for the granitic gneiss, tonalitic gneisses, and migmatitized tonalitic gneiss from the Taihua Complex within the Xiaoqinling terrane. This study aims to constrain the timing and magmatic processes of the Taihua Complex within the Xiaoqinling area, and through an integrated data of the Paleoproterozoic silicic magmatism (*ca.* 2.3–2.2 Ga) from across the craton to provide further in-

a a: Corresponding author:huichun@gs.ncku.edu.tw

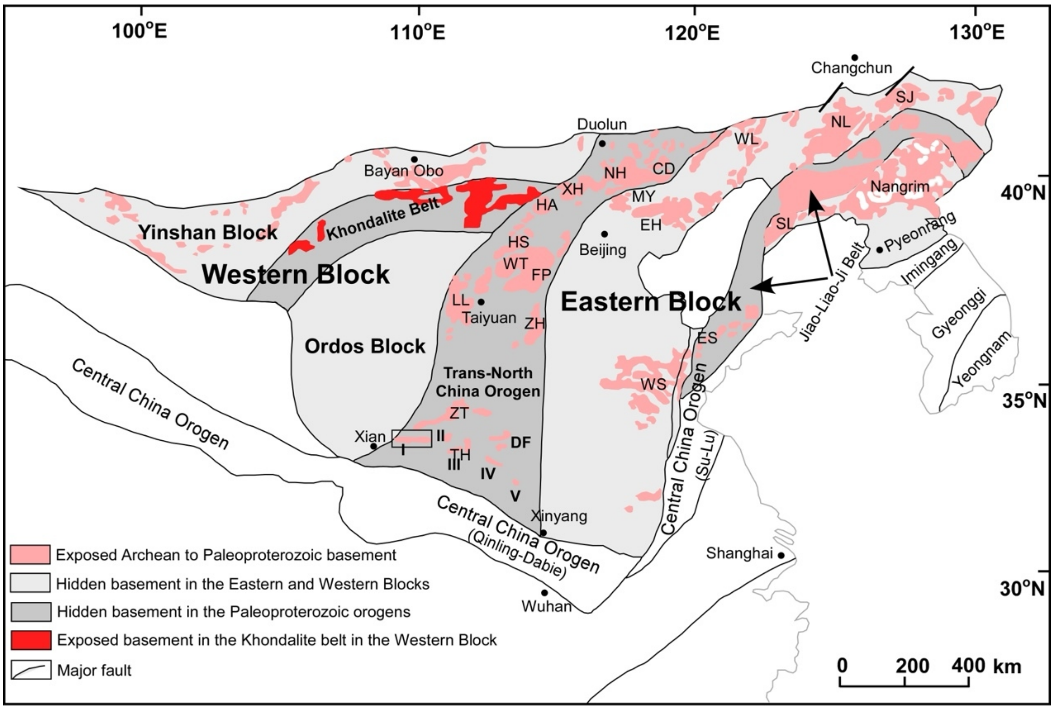

Figure 1. Geological sketch map of the North China Craton (NCC) (after Chen & Zhao, 2023). A square indicates the study area. Abbreviations: CD—Chengde; DF—Dengfeng; EH—Eastern Hebei; FP—Fuping; HA—Huai'an; HS—Hengshan; JD—Jiaodong; LL—Lvliang; NH—Northern Hebei; NL—Northern Liaoning; SJ—Southern Jilin; SL—Southern Liaoning; TH—Taihua; WL—Western Liaoning; WT—Wutai; WS—Western Shandong; XH—Xuanhua; ZH—Zanhuang; ZT—Zhongtiao. I to V refer to terranes in the Taihua complex: I. Xiaoqinling; II. Xiaoshan; III. Xiong'rshan; IV. Lushan; V. Wuyang.

sights into the Great Oxidation Event (GOE) and the global Huronian Glaciation Event (HGE).

2. GEOLOGICAL SETTINGS AND SAMPLES

2.1. North China Craton

The North China Craton (NCC) is an important tectonic unit, bordered by the globe's largest Phanerozoic accretionary orogen, the Central Asian Orogenic Belt to the north, and Central China Orogen to the south. Tectonically, the NCC can be divided into two major blocks named the Eastern and Western Blocks, separated by the Trans-North China Orogen (TNCO) which represents a *ca.* 1.85 Ga collision zone between the two blocks (fig. 1) (G. Zhao et al., 2001). The Western Block formed by amalgamation of the Yinshan Block in the north and the Ordos Block in the south along the Khondalite Belt at *ca.* 1.95 Ga (fig. 1) (G. Zhao et al., 2005). The Eastern Block underwent Paleoproterozoic (2.2–1.9Ga) rifting along its eastern continental margin, and the final closure of this rift system at *ca.*1.9 Ga led to the formation of the Jiao-Liao-Ji Belt (fig. 1) (G. Zhao et al., 2005). The basement of the NCC consists of variably exposed Archean to Paleoproterozoic rocks, including TTG gneiss, granite, charnockite, migmatite, amphibolite, ultramafite, mica schist, greenschist, Al-rich gneiss (khondalite), calcsilicate rock, banded iron formation (BIF), meta-arkose and marble, with a Mesoproterozoic to Phanerozoic cover (Jahn et al., 1987; Jahn & Zhang, 1984; Zhai, 2004).

2.2. Taihua Complex

The Taihua Complex, also termed the Taihua Group, is scattered along the southern margin of the TNCO from the Xiaoqinling, Xiaoshan, Xiong'ershan, Lushan, to Wuyang terranes (fig. 1). These five terranes may be part of the Qinling Orogen and hosted metalliferous deposits (Mao et al., 2002; Zhang et al., 2000).

2.3. Lithologies of the study area and sampling

The Taihua Complex within the Xiaoqinling terrane is the largest outcrop of Archean-Paleoproterozoic basement in the southern TNCO (fig. 1), which can be further subdivided into the lower and upper parts of the Taihua Complex. The lower part of the Taihua Complex mainly consists of tholeiite and tonalite-trondhjemite-granodiorite (TTG) suites metamorphosed into amphibolite and TTG gneiss, whereas the upper part of the Taihua Complex comprises quartzite, metapelitic gneiss and schist, marble and iron formation (Qi, 1992). According to earlier studies, the lithology of the Taihua Complex in the Xiaoqinling area can be further divided into four units: the *ca.* 2.8–2.2 Ga crystalline basement rocks that belong to the lower Taihua subgroup (X. Jia et al., 2016; Yu et al., 2013); the *ca.* 2.0–1.8 Ga metamorphic supracrustal rocks of the upper Taihua subgroup (Wan et al., 2006); the *ca.* 1.8–1.6 Ga sedimentary rocks covered

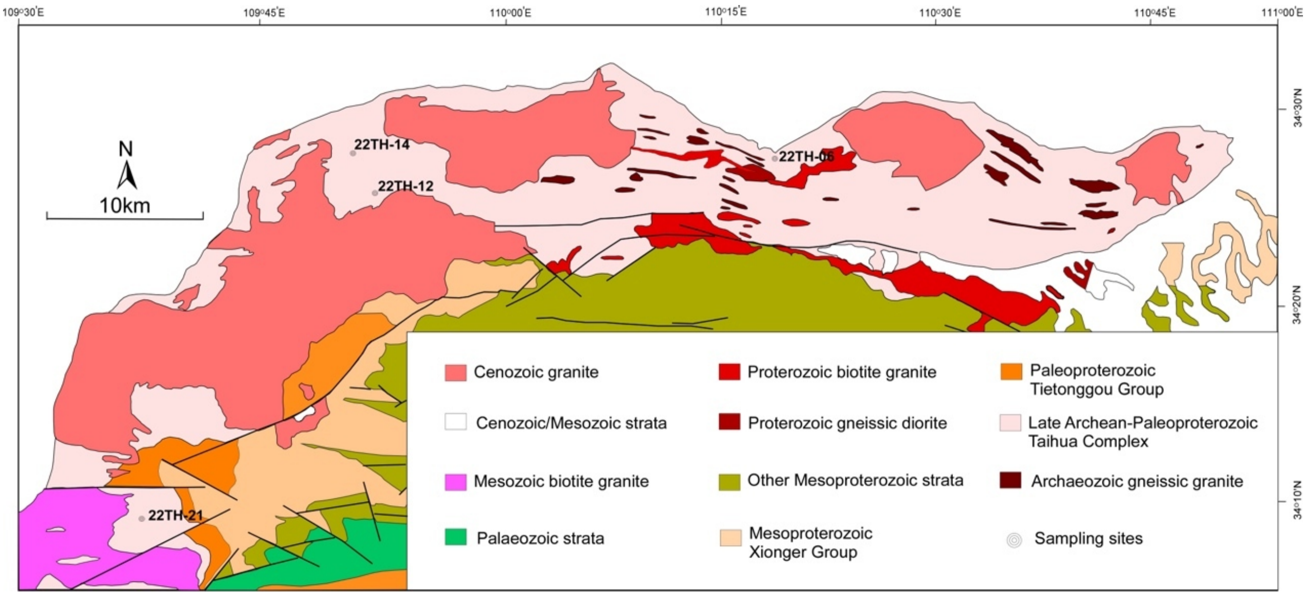

Figure 2. Simplified geological map of the Taihua Complex in the Xiaoqinling terrane, showing the sampling locations of U-Pb zircon dating and Hf-O isotopic study. (modified after the *Geological Bureau of Shaanxi Province*, 1966).

above the Taihua Complex (Diwu et al., 2013); and the *ca.* 160 Ma–110 Ma granite, which intrude into the Precambrian Complex in the region (Xu et al., 2009).

In this study, we collected representative granitic gneiss, tonalitic gneisses, and migmatitized tonalitic gneiss samples for geochronological and Lu-Hf and O isotopic analyses. The sampling locations are shown in figure 2, and their key information, including the coordinates, rock types, and mineral compositions, is listed in Supplementary Table S1. In the field, the grayish-white granitic gneiss (sample 22TH-06) (fig. 3A), collected from the Yushiyu section, Tongguan county, in the eastern part of the Xiaoqinling terrane, shows a granular granoblastic texture and a distinct gneissic structure, with nearly vertical foliation and oriented minerals such as quartz and feldspar. Most of the plagioclase grains are euhedral to subhedral in shape. The average quartz grains are larger than the feldspar grains. Samples 22TH-12 and 22TH-21 are two tonalitic gneisses collected some 0.9 km apart. These rocks are composed predominantly of quartz, feldspar, and biotite. The tonalitic gneiss (sample 22TH-12), collected from the Shaohuashan section in the central segment of the Xiaoqinling terrane, outcrops as river channel bedrock and is generally gray in color, showing a distinct gneissic structure with visible quartz, feldspar and biotite (fig. 3B). The tonalitic gneiss (sample 22TH-21), obtained from the Bayuan section in the western segment of the Xiaoqinling terrane, shows a pronounced orientation of quartz, feldspar and biotite in the field, with a gneissic foliation striking 175° and dipping 20° (fig. 3C). The tonalitic gneiss (sample 22TH-14), also collected from the Shaohuashan section in the central segment of the Xiaoqinling terrane, encloses blocks of amphibolite and exhibits local migmatization in the field, with small late-stage granitic veins intruding both the gneiss and the amphibolites (fig. 3D).

3. ANALYTICAL METHODS

Zircon cathodoluminescence (CL) images were obtained to reveal the internal texture of the grains, preparing for further zircon U-Pb age analyses and Hf-O isotopes. Cathodoluminescence (CL) images were taken by using a Scanning Electron Microscope (TESCAN MIRA 3) connected to a TESCAN MIRA 3 system, for examination of zircon internal structures and for selection of analytical spots.

Zircon U-Pb isotopic analysis was performed using a GeoLas HD laser ablation system combined with an Agilent 7900 quadrupole ICPMS (inductively coupled plasma mass spectrometer). A spot size of 32 μm with a laser repetition rate of 5 Hz was used, and the laser energy density was 5.5 J/cm^2. Zircon 91500 (Wiedenbeck et al., 1995) and synthetic silicate glass NIST610 (Jochum et al., 2011) were used as external standards for U-Pb dating and trace element calibration, respectively. Whereas zircons GJ-1 (Jackson et al., 2004), Tanz (Hu et al., 2021) and Plešovice (Sláma et al., 2008) were used for data quality control. Raw data were processed by using software ICPMSDataCal (Y. Liu et al., 2010). Detailed analytical results are presented in Supplementary Table S2. Concordia diagrams and ^{207}Pb/^{206}Pb age histograms were plotted using Isoplot/Ex_ver3 software (Ludwig, 2003).

In situ Lu-Hf isotopic analysis of zircon was performed using a 193 nm GeoLas HD excimer ArF laser ablation system (Coherent, Göttingen, Germany), attached to a Neptune Plus MC-ICP-MS (Thermo Fisher Scientific, Bremen, Germany). All analyses were carried out with a beam diameter of 44 μm, an 8 Hz repetition rate, and energy of 10 J/cm^2. Zircon standards Plešovice, GJ-1, and 91500 were analyzed after analysis every ten sample spots to ensure instrument stability and for data calibration (Morel et al., 2008). Detailed analytical results are presented in Supple-

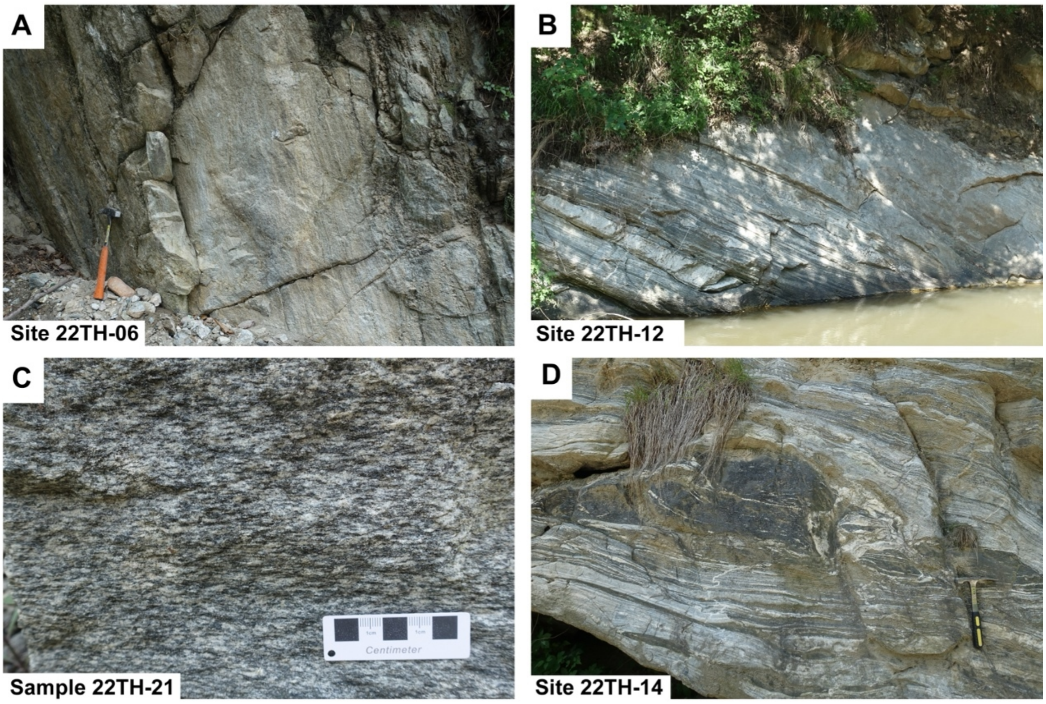

Figure 3. Photographs of metamorphic rocks outcropping in the study area: (A) granitic gneiss, site 22TH-06; (B) tonalitic gneiss, site 22TH-12; (C) tonalitic gneiss, sample 22TH-21; (D) migmatitized tonalitic gneiss, site 22TH-14.

mentary Table S3. Initial Hf isotopic ratios are recalculated to the determined ages, using the ^{176}Lu-^{176}Hf decay constant of 1.867 × 10^{-11} yr^{-1} (Söderlund et al., 2004). The values of εHf(t) are calculated relative to the chondritic reservoir with a ^{176}Hf/^{177}Hf ratio of 0.282772 and ^{176}Lu/^{177}Hf ratio of 0.0332 (Blichert-Toft & Albarède, 1997). Single-stage Hf mode ages (T_{DM1}) are calculated relative to the depleted mantle with a present-day value of ^{176}Hf/^{177}Hf = 0.28325, similar to that of average MORB (Nowell et al., 1998) and ^{176}Lu/^{177}Hf = 0.0384 (Griffin et al., 2000). Two-stage Hf model ages (T_{DM2}) are calculated by assuming a mean ^{176}Lu/^{177}Hf value of 0.015 for the average continental crust (Griffin et al., 2002).

Zircon oxygen isotope analysis was conducted using a CAMECA IMS 1300-HR^3 instrument. A primary 133Cs$^+$ ion beam (2.4–2.5 nA current and 20 keV total impact energy) was focused on the sample surface. A 5 μm × 5 μm raster was used in this study, and a normal-incidence electron gun was used for charge compensation. An NMR field sensor was applied to stabilize the magnetic field. The signals of ^{16}O and ^{18}O were collected simultaneously using two Faraday cups at positions L'2 and H'2, respectively. The L'2 and H'2 positions were configured with a resistor circuit of 10^{10} Ω and 10^{11} Ω, respectively. The mass resolving power (MRP, M/ΔM), measured at 50% peak height, was set at ~2500 to minimise isobaric interferences. The total analytical time was about 5 min per pit: 100 s pre-sputtering (to remove the Au coating); ~ 60 s automatic centering of the secondary ions in the field aperture, and a total of 80 s integration of secondary ions (twenty cycles × 4 s). To evaluate the reliability of the analytical protocols in this study, well-characterized zircon reference materials Penglai (X.-H. Li et al., 2010) and Qinghu (X. Li et al., 2013) were also analyzed. Detailed analytical results are presented in Supplementary Table S4.

4. RESULTS

4.1. Zircons from Granitic gneiss

Zircons from granitic gneiss 22TH-06 are colorless or dark gray, transparent to translucent, and oval or sub-rounded in shape. Grain length ranges from 80 to 220 μm, with length/width ratios of 1.5:1 to 3:1. Most of the zircons have sector or fir-tree zoning (fig. 4A), which is typical for metamorphic zircon (Corfu et al., 2003). Zircon U-Pb dating yields nearly concordant apparent U-Pb ages of 1894 ± 39 to 1781 ± 38 Ma (1SE) (Supplementary Table S2 and fig. 5A) with a weighted mean ^{207}Pb/^{206}Pb age of 1838 ± 18 Ma (2SE, n = 16, MSWD = 0.93), representing the metamorphic age. Ten analyses yield ^{176}Hf/^{177}Hf ratios vary from 0.281463–0.281498 (2SE), with corresponding negative εHf(t) values (−6.1 to −3.3), and Hf isotopic T_{DM2} model ages from 2883–2748 Ma (Supplementary Table S3). Fifteen O isotope analyses yield δ^{18}O values varying from 7.28 to 7.68‰ (2SE) (Supplementary Table S4).

4.2. Zircons from Tonalitic gneisses

Zircons from tonalitic gneiss 22TH-12 are generally dull gray to black, transparent to translucent, and oval or irregular in shape. Grain length ranges from 80 to 250 μm, with length/width ratios of 1.5:1 to 3:1. Zircon grains from this sample are subhedral to elliptical with clear core-rim struc-

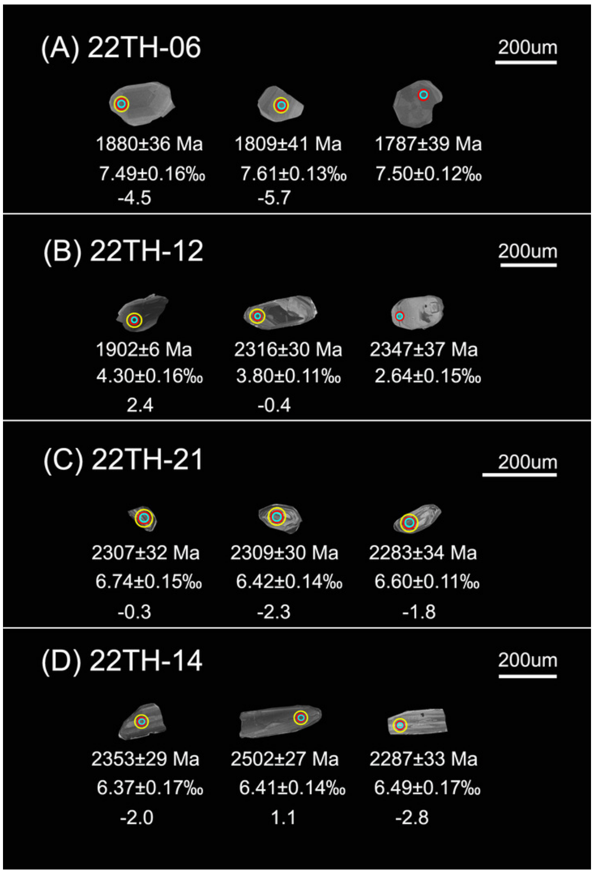

Figure 4. Representative Cathodoluminescence (CL) images of zircon grains from (A) granitic gneiss, (B) tonalitic gneiss, (C) tonalitic gneiss, (D) migmatitized tonalitic gneiss from the Taihua Complex within the Xiaoqinling terrane. Yellow circles indicate the Lu-Hf spots, red circles indicate the U-Pb spots, and blue circles denote the O isotope analysis spots.

tures (fig. 4B), which is characteristic of metamorphic zircon. The cores have euhedral to irregular shapes with oscillatory zones, while the broad rims are banded, or no zones (fig. 4B). Two concordant analyses yield concordia ages of *ca.* 1976–1902 Ma (1SE) ($^{207}Pb/^{206}Pb$ ages), indicating zircon recrystallization/regrowth during metamorphism. Zircon U-Pb dating yields nearly concordant apparent U-Pb ages of 2372 ± 28 to 2279 ± 33 Ma (1SE) (Supplementary Table S2 and fig. 5B) with a weighted mean $^{207}Pb/^{206}Pb$ age of 2328 ± 17 Ma (2SE, n = 13, MSWD = 0.8), representing its protolith age. Th/U ratios for the zircons vary from 0.19 to 0.72 consistent with igneous origin. In this sample, nine analyses of oscillatory zoned zircon cores have $\delta^{18}O$ values of 2.71–7.87‰ (2SE). These zircons have $^{176}Hf/^{177}Hf$ ratios between 0.281345 and 0.281405 (2SE), slightly negative to positive initial εHf(t) values (−0.8 to +2.1), and Hf isotopic T_{DM2} model ages from 2884–2739 Ma (Supplementary Table S3). Three metamorphic zircons (1976–1902 Ma) (1SE) have slightly lower $\delta^{18}O$ values of 4.30–4.54‰ (2SE) (Supplementary Table S4).

Zircons in tonalitic gneiss 22TH-21 are oval and elongate round, colorless and translucent. Grain length ranges from 40 to 150 m, with length/width ratios of 1.5:1 to 3:1. The zircon crystals occur as subhedral to euhedral grains. Most grains from this sample display a well-developed core-rim structure (fig. 4C). The zircon cores generally display oscillatory zoning or patchy zoning and some grains show very dark cores. The oscillatory zoning and high Th/U ratios (0.35–0.76) of these dated zircon cores are indicative of igneous origin and the obtained $^{207}Pb/^{206}Pb$ age of 2271±17 Ma (2SE) is interpreted as dating the crystallization of the protolith of the tonalitic gneiss (fig. 5C). Ten analyses yield $^{176}Hf/^{177}Hf$ ratios vary from 0.281276 to 0.281348 (2SE), with corresponding negative εHf(t) values (−3.0 to −0.3), and Hf isotopic T_{DM2} model ages from 2999–2870 Ma (Supplementary Table S3). Fifteen O isotope analyses yield $\delta^{18}O$ values varying from 6.35 to 6.85‰ (2SE) (Supplementary Table S4).

4.3. Zircons from Migmatitized Tonalitic gneiss

Zircons in migmatitized tonalitic gneiss 22TH-14 are generally colorless and translucent, and oval to irregular in shape. Grain length ranges from 40 to 250 μm, with length/width ratios of 1.5:1 to 5:1. Most of the grains have patchy zoning (fig. 4D), which is typical for metamorphic zircon (Corfu et al., 2003). Notably, some zircon exhibit micro-cracks and pseudo-inclusion, which were often observed in metamictization of zircons (K. Zhou et al., 2023). One nearly concordant spot has an age of 1820 ± 31 Ma (1SE) ($^{207}Pb/^{206}Pb$ age) (fig. 5D), which may be represented as the migmatization age. However, it is not likely to extract a reliable age of migmatitization from the data. Thirteen nearly concordant analyses yield $^{207}Pb/^{206}Pb$ ages of 2498–2287 Ma (1SE) (fig. 5D). The scatter is probably related to metamictization of the zircons and diffusional loss of radiogenic Pb. Collectively, the data suggest formation of the protolith from this sample at *ca.* 2498–2287 Ma (1SE), possible migmatitization and vein formation at *ca.* 1820 Ma (1SE). Ten analyses yield $^{176}Hf/^{177}Hf$ ratios vary from 0.281278 to 0.281449 (2SE), with εHf(t) values of −2.8 to +1.9, and Hf isotopic T_{DM2} model ages from 3018 to 2758 Ma (Supplementary Table S3). Fifteen O isotope analyses yield $\delta^{18}O$ values of 6.31 to 6.67‰ (2SE) (Supplementary Table S4).

5. DISCUSSION

5.1. Paleoproterozoic crustal evolution of the study region revealed by U-Pb-Hf-O isotopes

In the following section, we discuss zircon Hf-O isotopic signatures of the two main age groups of *ca.* 2.3–2.2 Ga and 1.8 Ga samples in this study and assess the origin and evolution of the Taihua metamorphic complex along the southern margin of the North China Craton (NCC).

The *ca.* 2498–2287 Ma migmatitized tonalitic gneiss sample 22TH-14 of the Taihua metamorphic complex defines the oldest protolith age in this study. It has crust-like Hf-O isotopic compositions with negative to positive εHf(t) (−2.8 – +1.9) and moderately elevated $\delta^{18}O$ values (6.31–6.67‰) (fig. 6), indicating the involvement of crustal components during magmatic crystallization. The $\delta^{18}O$

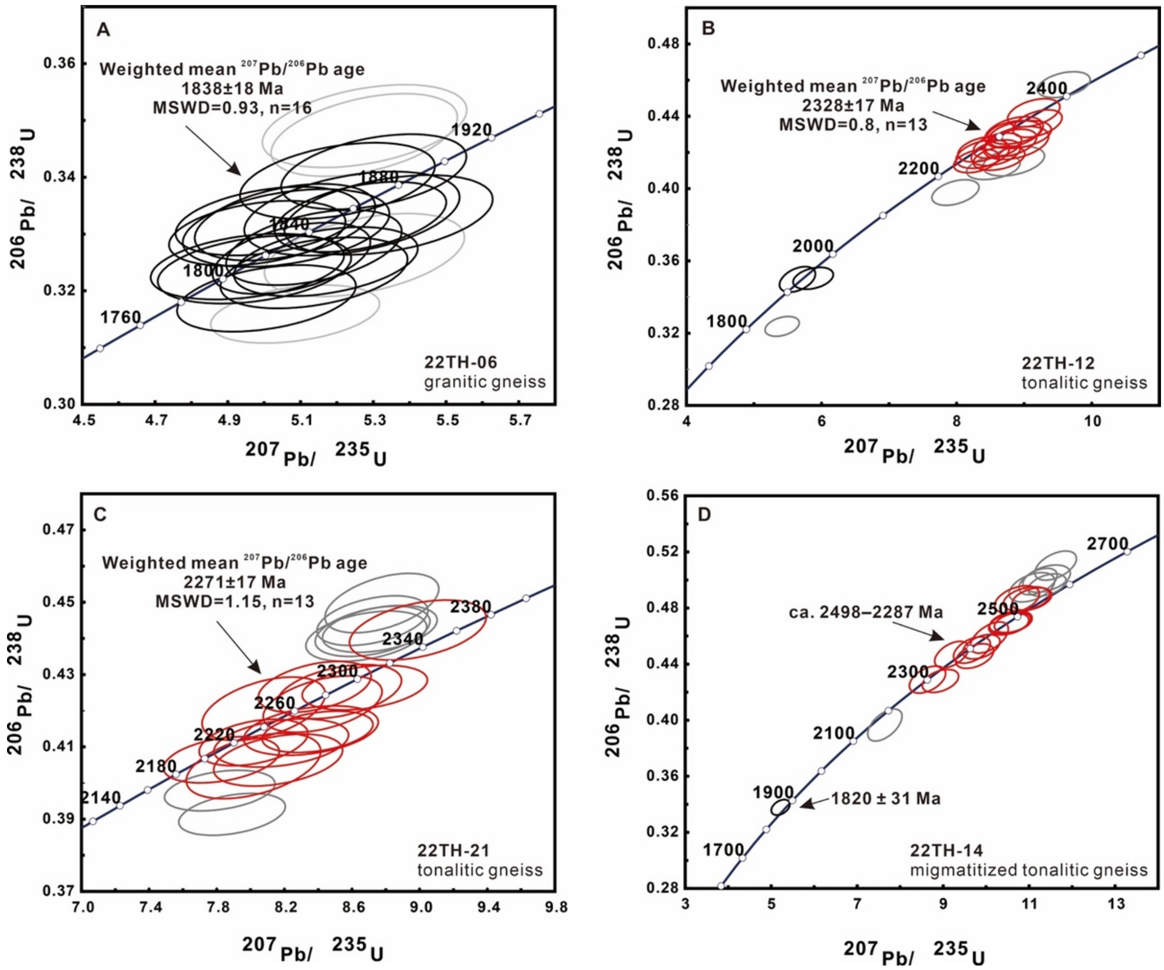

Figure 5. U-Pb concordia diagrams for metamorphic rock samples in this study. (A) granitic gneiss, sample 22TH-06; (B) tonalitic gneiss, sample 22TH-12; (C) tonalitic gneiss, sample 22TH-21; (D) migmatitized tonalitic gneiss, sample 22TH-14. Data-point error ellipses are 2SE and data-point error symbols are 2SE. Abbreviations: MSWD—mean square weighted deviation.

range is also similar for the I-type granite zircon values of 5.5 to 7.0 permil (Wörner et al., 1987). Thus, they are not primary melts directly from the depleted mantle but most likely have a mixed origin of continental crust assimilated by mantle-derived magmas.

Compared to the sample 22TH-14, the Hf isotopic compositions of *ca.* 2372–2279 Ma tonalitic gneiss (sample 22TH-12) from the bedrock of the river channel are more radiogenic with εHf(t) values of −0.8 to +2.1 (fig. 6A), indicating a juvenile input and a decrease crustal reworking. The zircons from this sample show a wide variation in $\delta^{18}O$ value: 2.71 to 7.87 permil, and most of them have $\delta^{18}O$ values lower than typical mantle zircon values of 5.3 ± 0.3 permil (1SD) (Valley et al., 2005).

Similar moderately elevated $\delta^{18}O$ values (6.35–6.85‰) were also observed for the tonalitic gneiss sample 22TH-21 (fig. 6B). Its protolith age at *ca.* 2309–2209 Ma with negative εHf(t) values of −3.0 to −0.3, which reflects that crustal reworking was dominant during their genesis.

The metamorphic age at *ca.* 1976–1902 Ma tonalitic gneiss (sample 22TH-12) with slightly positive εHf(t) and low $\delta^{18}O$ values (4.30–4.54‰) (fig. 6), which implies a hydrothermal alteration occurred. Based on theoretical calculations, high-T water-rock interaction is an important process to lower the oxygen isotope ratios of rocks and/or minerals (Z.-F. Zhao & Zheng, 2003). We may thus infer that this low $\delta^{18}O$ tonalitic gneiss can be formed by high-temperature hydrothermal alteration of surface water (seawater or meteoric water) (Bindeman & Valley, 2001; Zheng et al., 2004, 2008).

The metamorphic age at *ca.* 1894–1781 Ma granitic gneiss (sample 22TH-06) have negative εHf(t) values of −6.1 to −4.5 and relatively high $\delta^{18}O$ values (7.28–7.68‰) (fig. 6), which suggests that the recycled high $\delta^{18}O$ crustal material (Valley et al., 2009). Some zircons have elevated $\delta^{18}O$ (>7.5‰) due to melting of protoliths that were altered at low-temperature by hydrothermal reactions (Valley, 2003).

5.2. Comparison with Hf-O isotopic data of the Paleoproterozoic silicic magmatism at ca. 2.3–2.2 Ga in the NCC and further insights into the GOE and HGE

The Paleoproterozoic silicic magmatism occurred during the TML (*ca.* 2.3–2.2 Ga) (Condie et al., 2022). We compiled the Hf-O isotopic results of our samples with available pub-

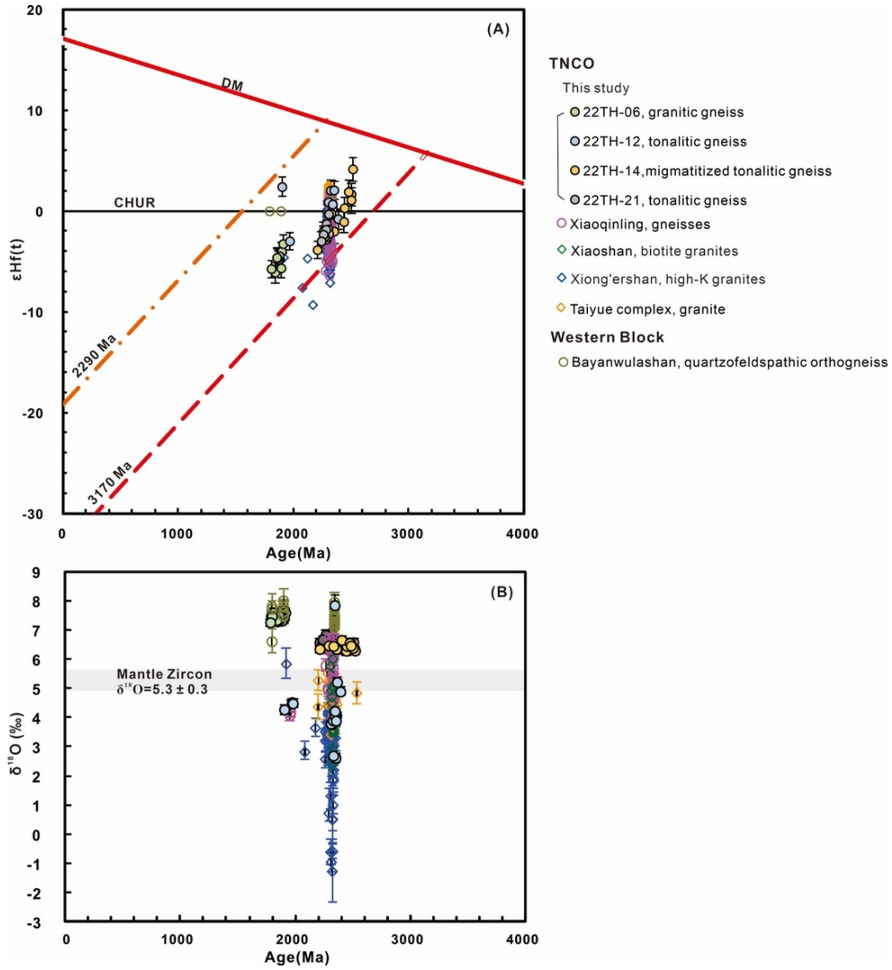

Figure 6. Composite plots of (A) Epsilon Hf(t) vs. U-Pb age for zircons from this study and comparative data from other regions of the NCC. Dashed lines show evolution of average continental crust, assuming $^{176}Lu/^{177}Hf$ = 0.015 (Griffin et al., 2002). Abbreviations: CHUR—chondrite uniform reservoir; DM—depleted mantle. (B) $\delta^{18}O$ vs. U-Pb age for zircons from this study and comparative data from other regions of the NCC. Data sources: This study; Xiong'ershan (Y. Zhou et al., 2021); Xiaoqinling (X. Wang et al., 2021); Xiaoshan (Sun et al., 2023); Taiyue complex (X. Wang et al., 2022); Bayanwulashan (Dan et al., 2012). Error bars are 2 SE.

lished data from granites and gneisses (protoliths) across the craton in the Bayanwulashan Complex of the Western Block, Taiyue Complex, and Taihua Complex of the Trans-North China Orogen (TNCO) during this period (fig. 6) (Dan et al., 2012; Sun et al., 2023; X. Wang et al., 2021, 2022; Y. Zhou et al., 2021).

In this study, the protolith of the tonalitic gneisses have crust-like Hf-O isotopic compositions with slightly negative to positive εHf(t) (−3.0– +2.1) and low to moderately elevated $\delta^{18}O$ values (2.71–7.87‰) (fig. 6), suggesting the involvement of crustal components during magmatic crystallization. Our results imply that they are not primary melts directly from the depleted mantle but most likely have a mixed origin of continental crust assimilated by mantle-derived magmas. Based on previous study (X. Wang et al., 2021), the gneisses in the Xiaoqinling terrane show a relatively wide range of Hf isotopic values from −6.4 to +1.9 (fig. 6), indicating various contributions from multiple mantle- and crust-derived components. Similar low to moderately elevated $\delta^{18}O$ values (3.97–6.79‰) has also been observed, which may represent the high-temperature hydrothermal alteration. The quartzofeldspathic orthogneiss in the Bayanwulashan Complex (Dan et al., 2012) has slightly negative to positive εHf(t) (−0.7 to +1.0) and moderate $\delta^{18}O$ value of 7.12–7.98‰ (fig. 6), which indicates that juvenile inputs during their genesis and low-temperature hydrothermal alteration might have occurred. The biotite granite in the Xiaoshan terrane (Sun et al., 2023) displays slightly negative to positive εHf(t) (−1.1 to +1.4) and low to moderately elevated $\delta^{18}O$ values of 2.41–6.04‰ (fig. 6). Compared to the biotite granite in the Xiaoshan terrane, the granite in the Taiyue complex (X. Wang et al., 2022) has similar Hf-O isotopic compositions, with slightly negative to positive εHf(t) (−1.6 to +2.6) and low $\delta^{18}O$ values of 3.29–5.53‰ (fig. 6). The high-K granites in the Xiong'ershan terrane (Y. Zhou et al., 2021) show negative εHf(t) (−9.3 to −1.1) and slightly negative to low $\delta^{18}O$ values (−1.24–4.78‰), which indicating that crustal reworking was dominant during their genesis associated with high-temperature hydrothermal alteration of surface water.

As the most significant event in the early Paleoproterozoic, the Great Oxidation Event (GOE), is known for the dramatic change in atmospheric composition where the free oxygen in the atmosphere increased by nearly five orders of magnitude, a likely response to biogeochemical feedbacks linked to the evolution of photosynthesizing bacteria (Kump, 2008). Extreme environmental changes greatly affected ocean and atmosphere chemistry. Tang and Chen (2013) proposed a two-stage oxygenation model for the GOE, which includes the early-stage hydrosphere oxidation (2.5–2.3 Ga) and the late-stage atmospheric oxygenation (2.3– 2.2 Ga). After 2.3 Ga, increasing O_2 and decreasing CH_4 and CO_2, the icehouse effect of O_2 cooled the climate and resulted in the global Huronian Glaciation Event (HGE, 2.29–2.25 Ga) (Hoffman, 2013; Tang & Chen, 2013).

Integration of our new U-Pb and Hf-O isotope data with available published data of the NCC of this period (*ca.* 2.3–2.2 Ga) (Supplementary Table S5), indicating that most of the magma source(s) at the Taiyue Complex, and Taihua Complex (e.g., Xiaoqinling, Xiaoshan, and Xiong'rshan areas) in the southern TNCO, which were likely formed by high-temperature hydrothermal alteration of surface water (at *ca.* 2.3 Ga). In contrast, the magma source(s) at the Bayanwulashan Complex of the Western Block experienced low-temperature hydrothermal reactions at roughly the same time. The protolith of the gneisses (2.32 to 2.21 Ga) were occurred in the Xiaoqinling area does appear in which temporal coincidence with the HGE. It is noteworthy that at *ca.* 2.2 Ga, the Taihua Complex within the Xiaoqinling area underwent low-temperature hydrothermal reactions during the magmatic crystallization, which might have affected by the HGE. However, further study will be needed to reveal the mechanisms.

6. CONCLUSIONS

Based on the new data presented in this study and in combination with previous studies, we can draw the following conclusions:

1. The protolith of the tonalitic gneisses in the study area have crust-like Hf-O isotopic compositions with slightly negative to positive εHf(t) (−3.0– +2.1) and low to moderately elevated $\delta^{18}O$ values (2.71–7.87‰), indicating a mixed origin of continental crust assimilated by mantle-derived magmas.
2. Low $\delta^{18}O$ values suggest that the protolith of the tonalitic gneisses in the Taihua Complex within the Xiaoqinling area was likely formed by high-temperature hydrothermal alteration of surface water. The granitic gneiss in the study area has elevated $\delta^{18}O$ (>7.5‰), which underwent low-temperature hydrothermal reactions.
3. The study area underwent low-temperature hydrothermal reactions during the magmatic crystallization at *ca.* 2.2 Ga, which might have been affected by the HGE. However, further study will be needed to reveal the mechanisms.

Acknowledgments

This research was financially supported by the National Science and Technology Council (NSTC) in Taiwan, under Grant NSTC111-2636-M-006-019 and NSTC112-2116-M-006-005-MY2. We thank Xin Zhu, Rutao Zang, Fubao Chong, and Qingxing Luo for assistance in the field excursion. We also thank two anonymous reviewers for their suggestions in the revision process.

Author Contributions

Nancy Hui-Chun Chen: Writing – review & editing, Writing –original draft, Visualization, Validation, Methodology, Investigation, Funding acquisition, Formal analysis, Data curation, Conceptualization. **Yunpeng Dong:** Investigation. **Bo Hui:** Investigation.

Data and Supplementary Information

Supplementary Tables S1–S5 are available: https://doi.org/10.17632/zpyp4rmb43.1

Competing Interests

The authors declare no competing financial interests.

Editor: Mark Brandon, Associate Editor: Guochun Zhao

Submitted: January 19, 2024 EST, Accepted: September 14, 2024 EST

REFERENCES

Bindeman, I. N., & Valley, J. W. (2001). Low-δ^{18}O rhyolites from Yellowstone: Magmatic evolution based on analyses of zircons and individual phenocrysts. *Journal of Petrology*, *42*(8), 1491–1517. https://doi.org/10.1093/petrology/42.8.1491

Blichert-Toft, J., & Albarède, F. (1997). The Lu-Hf isotope geochemistry of chondrites and the evolution of the mantle-crust system. *Earth and Planetary Science Letters*, *148*(1–2), 243–258. https://doi.org/10.1016/s0012-821x(97)00040-x

Chen, N. H.-C., & Zhao, G. (2023). Detrital zircons from Paleoproterozoic (meta-)sedimentary rocks on the northern margin of the North China Craton and tectonic implications. *Precambrian Research*, *384*, 106946. https://doi.org/10.1016/j.precamres.2022.106946

Condie, K. C., Pisarevsky, S. A., Puetz, S. J., Spencer, C. J., Teixeira, W., & Faleiros, F. M. (2022). A reappraisal of the global tectono-magmatic lull at~ 2.3 Ga. *Precambrian Research*, *376*, 106690. https://doi.org/10.1016/j.precamres.2022.106690

Corfu, F., Hanchar, J. M., Hoskin, P. W., & Kinny, P. (2003). Atlas of zircon textures. *Reviews in Mineralogy and Geochemistry*, *53*(1), 469–500. https://doi.org/10.2113/0530469

Dan, W., Li, X. H., Guo, J., Liu, Y., & Wang, X.-C. (2012). Paleoproterozoic evolution of the eastern Alxa Block, westernmost North China: Evidence from in situ zircon U-Pb dating and Hf-O isotopes. *Gondwana Research*, *21*(4), 838–864. https://doi.org/10.1016/j.gr.2011.09.004

Diwu, C., Sun, Y., Gao, J., & Fan, L. (2013). Early Precambrian tectonothermal events of the North China Craton: Constraints from in situ detrital zircon U-Pb, Hf and O isotopic compositions in Tietonggou Formation. *Chinese Science Bulletin*, *58*(31), 3760–3770. https://doi.org/10.1007/s11434-013-5817-z

Diwu, C., Sun, Y., Zhao, Y., & Lai, S. (2014). Early Paleoproterozoic (2.45–2.20 Ga) magmatic activity during the period of global magmatic shutdown: Implications for the crustal evolution of the southern North China Craton. *Precambrian Research*, *255*, 627–640. https://doi.org/10.1016/j.precamres.2014.08.001

Geological Bureau of Shaanxi Province. (1966).

Griffin, W. L., Pearson, N. J., Belousova, E., Jackson, S. E., van Achterbergh, E., O'Reilly, S. Y., & Shee, S. R. (2000). The Hf isotope composition of cratonic mantle: LAM-MC-ICPMS analysis of zircon megacrysts in kimberlites. *Geochimica et Cosmochimica Acta*, *64*(1), 133–147. https://doi.org/10.1016/s0016-7037(99)00343-9

Griffin, W. L., Wang, X., Jackson, S. E., Pearson, N. J., O'Reilly, S. Y., Xu, X., & Zhou, X. (2002). Zircon chemistry and magma mixing, SE China: in-situ analysis of Hf isotopes, Tonglu and Pingtan igneous complexes. *Lithos*, *61*(3–4), 237–269. https://doi.org/10.1016/s0024-4937(02)00082-8

Hoffman, P. F. (2013). The Great Oxidation and a Siderian snowball Earth: MIF-S based correlation of Paleoproterozoic glacial epochs. *Chemical Geology*, *362*, 143–156. https://doi.org/10.1016/j.chemgeo.2013.04.018

Hu, Z., Li, X.-H., Luo, T., Zhang, W., Crowley, J., Li, Q., Ling, X., Yang, C., Li, Y., Feng, L., Xia, X., Zhang, S.-B., Wang, Z., Guo, J., Xu, L., Lin, J., Liu, X., Bao, Z., Liu, Y., & Hu, S. (2021). Tanz zircon megacrysts: a new zircon reference material for the microbeam determination of U-Pb ages and Zr-O isotopes. *Journal of Analytical Atomic Spectrometry*, *36*(12), 2715–2734. https://doi.org/10.1039/d1ja00311a

Huang, X.-L., Wilde, S. A., Yang, Q.-J., & Zhong, J.-W. (2012). Geochronology and petrogenesis of gray gneisses from the Taihua Complex at Xiong'er in the southern segment of the Trans-North China Orogen: Implications for tectonic transformation in the Early Paleoproterozoic. *Lithos*, *134–135*, 236–252. https://doi.org/10.1016/j.lithos.2012.01.004

Jackson, S. E., Pearson, N. J., Griffin, W. L., & Belousova, E. A. (2004). The application of laser ablation-inductively coupled plasma-mass spectrometry to in situ U–Pb zircon geochronology. *Chemical Geology*, *211*(1–2), 47–69. https://doi.org/10.1016/j.chemgeo.2004.06.017

Jahn, B. M., Auvray, B., Cornichet, J., Bai, Y. L., Shen, Q. H., & Liu, D. Y. (1987). 3.5 Ga old amphibolites from eastern Hebei Province, China: field occurrence, petrography, Sm-Nd isochron age and REE geochemistry. *Precambrian Research*, *34*(3–4), 311–346. https://doi.org/10.1016/0301-9268(87)90006-4

Jahn, B. M., & Zhang, Z. -q. (1984). Archean granulite gneisses from eastern Hebei Province, China: rare earth geochemistry and tectonic implications. *Contributions to Mineralogy and Petrology*, *85*(3), 224–243. https://doi.org/10.1007/bf00378102

Jia, X., Zhu, X., Zhai, M., Zhao, Y., Zhang, H., Wu, J., & Liu, T. (2016). Late Mesoarchean crust growth event: evidence from the ca. 2.8 Ga granodioritic gneisses of the Xiaoqinling area, southern North China Craton. *Science Bulletin*, *61*(12), 974–990. https://doi.org/10.1007/s11434-016-1094-y

Jia, X.-L., Zhai, M.-G., Xiao, W. -j., Sun, Y., Ratheesh-Kumar, R. T., Yang, H., Zhou, K.-F., & Wu, J.-L. (2019). Late Neoarchean to early Paleoproterozoic tectonic evolution of the southern North China Craton: Evidence from geochemistry, zircon geochronology and Hf isotopes of felsic gneisses from the Taihua complex. *Precambrian Research*, *326*, 222–239. https://doi.org/10.1016/j.precamres.2017.11.013

Jochum, K. P., Weis, U., Stoll, B., Kuzmin, D., Yang, Q., Raczek, I., Jacob, D. E., Stracke, A., Birbaum, K., Frick, D. A., Günther, D., & Enzweiler, J. (2011). Determination of Reference Values for NIST SRM 610-617 Glasses Following ISO Guidelines. *Geostandards and Geoanalytical Research*, *35*(4), 397–429. https://doi.org/10.1111/j.1751-908x.2011.00120.x

Kump, L. R. (2008). The rise of atmospheric oxygen. *Nature*, *451*(7176), 277–278. https://doi.org/10.1038/nature06587

Li, X., Tang, G., Gong, B., Yang, Y., Hou, K., Hu, Z., Li, Q., Liu, Y., & Li, W. (2013). Qinghu zircon: A working reference for microbeam analysis of U-Pb age and Hf and O isotopes. *Chinese Science Bulletin*, *58*(36), 4647–4654. https://doi.org/10.1007/s11434-013-5932-x

Li, X.-H., Long, W.-G., Li, Q.-L., Liu, Y., Zheng, Y.-F., Yang, Y.-H., Chamberlain, K. R., Wan, D.-F., Guo, C.-H., Wang, X.-C., & Tao, H. (2010). Penglai Zircon Megacrysts: A Potential New Working Reference Material for Microbeam Determination of Hf-O Isotopes and U-Pb Age. *Geostandards and Geoanalytical Research*, *34*(2), 117–134. https://doi.org/10.1111/j.1751-908x.2010.00036.x

Li, Y., Zhu, G., Gu, C., Su, N., Xiao, S., Zhang, S., Liu, C., & Xie, C. (2018). Structural evolution of the Paleoproterozoic Trans-North China Orogen: Evidence from the Xiaoqinling region, central China. *Precambrian Research*, *316*, 244–274. https://doi.org/10.1016/j.precamres.2018.08.020

Liu, D. Y., Nutman, A. P., Compston, W., Wu, J. S., & Shen, Q. H. (1992). Remnants of ≥3800 Ma crust in the Chinese part of the Sino-Korean craton. *Geology*, *20*(4), 339. https://doi.org/10.1130/0091-7613(1992)020

Liu, Y., Hu, Z., Zong, K., Gao, C., Gao, S., Xu, J., & Chen, H. (2010). Reappraisement and refinement of zircon U-Pb isotope and trace element analyses by LA-ICP-MS. *Chinese Science Bulletin*, *55*(15), 1535–1546. https://doi.org/10.1007/s11434-010-3052-4

Ludwig, K. R. (2003). *Isoplot/Ex version 3.00. A Geochronological Toolkit for Microsoft Excel, User's Manual* (pp. 1–70). Berkeley Geochronology Center Special Publications.

Mao, J., Goldfarb, R., Zhang, Z., Xu, W., Qiu, Y., & Deng, J. (2002). Gold deposits in the Xiaoqinling-Xiong'ershan region, Qinling Mountains, central China. *Mineralium Deposita*, *37*(3–4), 306–325. https://doi.org/10.1007/s00126-001-0248-1

Morel, M. L. A., Nebel, O., Nebel-Jacobsen, Y. J., Miller, J. S., & Vroon, P. Z. (2008). Hafnium isotope characterization of the GJ-1 zircon reference material by solution and laser-ablation MC-ICPMS. *Chemical Geology*, *255*(1–2), 231–235. https://doi.org/10.1016/j.chemgeo.2008.06.040

Nowell, G. M., Kempton, P. D., Noble, S. R., Fitton, J. G., Saunders, A. D., Mahoney, J. J., & Taylor, R. N. (1998). High precision Hf isotope measurements of MORB and OIB by thermal ionisation mass spectrometry: insights into the depleted mantle. *Chemical Geology*, *149*(3–4), 211–233. https://doi.org/10.1016/s0009-2541(98)00036-9

Partin, C. A., Bekker, A., Sylvester, P. J., Wodicka, N., Stern, R. A., Chacko, T., & Heaman, L. M. (2014). Filling in the juvenile magmatic gap: Evidence for uninterrupted Paleoproterozoic plate tectonics. *Earth and Planetary Science Letters*, *388*, 123–133. https://doi.org/10.1016/j.epsl.2013.11.041

Qi, J. (1992). Metamorphic rock series of Taihua Group and conditions for its formation in eastern Qinling. *Scientia Geologica Sinica*, *27*, 94–107.

Scaillet, B., Holtz, F., & Pichavant, M. (2016). Experimental constraints on the formation of silicic magmas. *Elements*, *12*(2), 109–114. https://doi.org/10.2113/gselements.12.2.109

Sláma, J., Košler, J., Condon, D. J., Crowley, J. L., Gerdes, A., Hanchar, J. M., Horstwood, M. S. A., Morris, G. A., Nasdala, L., Norberg, N., Schaltegger, U., Schoene, B., Tubrett, M. N., & Whitehouse, M. J. (2008). Plešovice zircon — A new natural reference material for U-Pb and Hf isotopic microanalysis. *Chemical Geology*, *249*(1–2), 1–35. https://doi.org/10.1016/j.chemgeo.2007.11.005

Söderlund, U., Patchett, P. J., Vervoort, J. D., & Isachsen, C. E. (2004). The 176Lu decay constant determined by Lu-Hf and U-Pb isotope systematics of Precambrian mafic intrusions. *Earth and Planetary Science Letters*, *219*(3–4), 311–324. https://doi.org/10.1016/s0012-821x(04)00012-3

Sun, Q., Zhao, T., Zhou, J., Wu, Z., & Zhou, Y. (2023). Petrogenesis of the ca. 2.32 Ga low-δ18O gabbroic diorites and granites in the Xiaoshan area, southern North China Craton: Implications for the early Paleoproterozoic tectonic evolution. *Precambrian Research*, *384*, 106924. https://doi.org/10.1016/j.precamres.2022.106924

Tang, H., & Chen, Y. (2013). Global glaciations and atmospheric change at ca. 2.3 Ga. *Geoscience Frontiers*, *4*(5), 583–596. https://doi.org/10.1016/j.gsf.2013.02.003

Taylor, H. P., Jr., & Sheppard, S. M. (1986). Igneous rocks; I, Processes of isotopic fractionation and isotope systematics. *Reviews in Mineralogy and Geochemistry*, *16*, 227–271. https://doi.org/10.1515/9781501508936-013

Teixeira, W., Ávila, C., Dussin, I., Neto, A. C., Bongiolo, E., Santos, J., & Barbosa, N. (2015). A juvenile accretion episode (2.35-2.32 Ga) in the Mineiro belt and its role to the Minas accretionary orogeny: Zircon U-Pb-Hf and geochemical evidences. *Precambrian Research*, *256*, 148–169. https://doi.org/10.1016/j.precamres.2014.11.009

Valley, J. W. (2003). Oxygen isotopes in zircon. *Reviews in Mineralogy and Geochemistry*, *53*(1), 343–385. https://doi.org/10.2113/0530343

Valley, J. W., Kita, N. T., & Fayek, M. (2009). In situ oxygen isotope geochemistry by ion microprobe. *MAC Short Course: Secondary Ion Mass Spectrometry in the Earth Sciences*, *41*, 19–63. http://www.geology.wisc.edu/zircon/new_tech/Valley%26Kita2009.pdf

Valley, J. W., Lackey, J. S., Cavosie, A. J., Clechenko, C. C., Spicuzza, M. J., Basei, M. A. S., Bindeman, I. N., Ferreira, V. P., Sial, A. N., King, E. M., Peck, W. H., Sinha, A. K., & Wei, C. S. (2005). 4.4 billion years of crustal maturation: oxygen isotope ratios of magmatic zircon. *Contributions to Mineralogy and Petrology*, *150*(6), 561–580. https://doi.org/10.1007/s00410-005-0025-8

Wan, Y., Wilde, S. A., Liu, D., Yang, C., Song, B., & Yin, X. (2006). Further evidence for~ 1.85 Ga metamorphism in the Central Zone of the North China Craton: SHRIMP U–Pb dating of zircon from metamorphic rocks in the Lushan area, Henan Province. *Gondwana Research*, *9*(1–2), 189–197. https://doi.org/10.1016/j.gr.2005.06.010

Wang, G.-D., Wang, H. Y. C., Chen, H.-X., Zhang, B., Zhang, Q., & Wu, C.-M. (2017). Geochronology and geochemistry of the TTG and potassic granite of the Taihua complex, Mts. Huashan: Implications for crustal evolution of the southern North China Craton. *Precambrian Research*, *288*, 72–90. https://doi.org/10.1016/j.precamres.2016.11.006

Wang, X., Huang, X.-L., & Yang, F. (2019). Revisiting the Lushan-Taihua Complex: New perspectives on the Late Mesoarchean-Early Neoarchean crustal evolution of the southern North China Craton. *Precambrian Research*, *325*, 132–149. https://doi.org/10.1016/j.precamres.2019.02.020

Wang, X., Huang, X.-L., & Yang, F. (2021). Geochronology and geochemistry of the Xiaoqinling Taihua Complex in the southern Trans-North China Orogen: Implications for magmatism during the early Paleoproterozoic global tectono-magmatic shutdown. *Lithos*, *402–403*, 106248. https://doi.org/10.1016/j.lithos.2021.106248

Wang, X., Zhu, W.-B., Zheng, Y.-F., & Ge, R.-F. (2022). Tectonic switch from a lithospheric rift to an active continental margin in the Paleoproterozoic: Evidence from low $\delta^{18}O$ granites from the Trans-North China Orogen in the North China Craton. *Precambrian Research*, *377*, 106672. https://doi.org/10.1016/j.precamres.2022.106672

Wiedenbeck, M., Allé, P., Corfu, F. Y., Griffin, W. L., Meier, M., Oberli, F. V., Roddick, J. C., & Spiegel, W. (1995). Three natural zircon standards for U-Th-Pb, Lu-Hf, trace element and REE analyses. *Geostandards Newsletter*, *19*(1), 1–23. https://doi.org/10.1111/j.1751-908X.1995.tb00147.x

Wörner, G., Harmon, R., & Hoefs, J. (1987). Stable isotope relations in an open magma system, Laacher See, Eifel (FRG). *Contributions to Mineralogy and Petrology*, *95*(3), 343–349. https://doi.org/10.1007/bf00371848

Xu, X., Griffin, W. L., Ma, X., O'Reilly, S. Y., He, Z., & Zhang, C. (2009). The Taihua group on the southern margin of the North China craton: further insights from U-Pb ages and Hf isotope compositions of zircons. *Mineralogy and Petrology*, *97*(1–2), 43–59. https://doi.org/10.1007/s00710-009-0062-5

Yu, X., Liu, J., Li, C., Chen, S., & Dai, Y. (2013). Zircon U-Pb dating and Hf isotope analysis on the Taihua Complex: constraints on the formation and evolution of the Trans-North China Orogen. *Precambrian Research*, *230*, 31–44. https://doi.org/10.1016/j.precamres.2012.12.008

Zhai, M. (2004). Precambrian tectonic evolution of the North China Craton. *Geological Society, London, Special Publications*, *226*(1), 57–72. https://doi.org/10.1144/gsl.sp.2004.226.01.04

Zhang, G. W., Yu, Z. P., Dong, Y. P., & Yao, A. P. (2000). On Precambrian framework and evolution of the Qinling belt. *Acta Petrologica Sinica*, *16*(1), 11–21.

Zhao, G., Sun, M., Wilde, S. A., & Sanzhong, L. (2005). Late Archean to Paleoproterozoic evolution of the North China Craton: key issues revisited. *Precambrian Research*, *136*(2), 177–202. https://doi.org/10.1016/j.precamres.2004.10.002

Zhao, G., Wilde, S. A., Cawood, P. A., & Sun, M. (2001). Archean blocks and their boundaries in the North China Craton: lithological, geochemical, structural and P-T path constraints and tectonic evolution. *Precambrian Research*, *107*(1–2), 45–73. https://doi.org/10.1016/s0301-9268(00)00154-6

Zhao, Z.-F., & Zheng, Y.-F. (2003). Calculation of oxygen isotope fractionation in magmatic rocks. *Chemical Geology*, *193*(1–2), 59–80. https://doi.org/10.1016/s0009-2541(02)00226-7

Zheng, Y.-F., Wu, R.-X., Wu, Y.-B., Zhang, S.-B., Yuan, H., & Wu, F.-Y. (2008). Rift melting of juvenile arc-derived crust: Geochemical evidence from Neoproterozoic volcanic and granitic rocks in the Jiangnan Orogen, South China. *Precambrian Research*, *163*(3–4), 351–383. https://doi.org/10.1016/j.precamres.2008.01.004

Zheng, Y.-F., Wu, Y.-B., Chen, F.-K., Gong, B., Li, L., & Zhao, Z.-F. (2004). Zircon U-Pb and oxygen isotope evidence for a large-scale ^{18}O depletion event in igneous rocks during the Neoproterozoic. *Geochimica et Cosmochimica Acta*, *68*(20), 4145–4165. https://doi.org/10.1016/j.gca.2004.01.007

Zhou, K., Chen, Y.-X., Xiong, J.-W., Schertl, H.-P., & Xia, X.-P. (2023). Fluid effect on zircon O and U-Pb isotopes during ultrahigh-pressure metamorphism: Insights from the Dora-Maira Massif of the Western Alps. *Geoscience Frontiers*, *14*(6), 101651. https://doi.org/10.1016/j.gsf.2023.101651

Zhou, Y., Sun, Q., Zhao, T., & Diwu, C. (2016). The Paleoproterozoic continental evolution in the southern North China Craton: Constrains from magmatism and sedimentation. In M. Zhai, Y. Zhao, & T. Zhao (Eds.), *Main Tectonic Events and Metallogeny of the North China Craton*. Springer. https://doi.org/10.1007/978-981-10-1064-4_10

Zhou, Y., Sun, Q., Zhao, T., & Zhai, M. (2021). Petrogenesis of the early Paleoproterozoic low-$\delta^{18}O$ potassic granites in the southern NCC and its possible implications for no confluence of glaciations and magmatic shutdown at ca. 2.3 Ga. *Precambrian Research*, *361*, 106258. https://doi.org/10.1016/j.precamres.2021.106258

SUPPLEMENTARY MATERIALS

Summary of the samples and sampling positions in this study.

Download: https://ajsonline.org/article/123684-zircon-u-pb-age-and-hf-o-isotope-evidence-of-the-taihua-complex-on-the-southern-margin-of-the-north-china-craton-implications-for-its-magmatic-proces/attachment/246586.docx

U-Pb age data for zircons of metamorphic rocks in this study.

Download: https://ajsonline.org/article/123684-zircon-u-pb-age-and-hf-o-isotope-evidence-of-the-taihua-complex-on-the-southern-margin-of-the-north-china-craton-implications-for-its-magmatic-proces/attachment/246587.docx

Zircon Lu-Hf isotopic compositions of metamorphic rocks in this study.

Download: https://ajsonline.org/article/123684-zircon-u-pb-age-and-hf-o-isotope-evidence-of-the-taihua-complex-on-the-southern-margin-of-the-north-china-craton-implications-for-its-magmatic-proces/attachment/246588.docx

Zircon O isotopes of metamorphic rocks in this study.

Download: https://ajsonline.org/article/123684-zircon-u-pb-age-and-hf-o-isotope-evidence-of-the-taihua-complex-on-the-southern-margin-of-the-north-china-craton-implications-for-its-magmatic-proces/attachment/246589.docx

Compilation of zircon U-Pb ages and Hf-O isotopic data of the North China Craton during the ~2.3–2.2 Ga.

Download: https://ajsonline.org/article/123684-zircon-u-pb-age-and-hf-o-isotope-evidence-of-the-taihua-complex-on-the-southern-margin-of-the-north-china-craton-implications-for-its-magmatic-proces/attachment/246590.docx